J Fusion Energ
DOI 10.1007/s10894-013-9658-1

ORIGINAL RESEARCH

Some Generalised Characteristics of the Electro-dynamics of the Plasma Focus in Its Axial Phase: Illustrated by an Application to Independantly Determine the Drive Current Fraction and the Mass Swept-Up Fraction

S. Lee · S. H. Saw · H. Hegazy · Jalil Ali · V. Damideh · N. Fatis · H. Kariri · A. Khabrani · A. Mahasi

Abstract We describe the axial phase of the Mather plasma focus by two coupled equations of motion and circuit. We non-dimensionalised these equations resulting in two coupled equations which are characterised by only three scaling parameters α, β and δ which are ratios of electrical to transit times, inductances and impedances respectively. The normalised current waveform, trajectory and speed profile are unique for each combination of α, β, δ which are the ratios of characteristic times (electrical discharge vs. axial transit), inductances (tube inductance vs. static inductance) and impedances (stray resistance vs. electrical surge impedance). This leads to important information and insight into various aspects of the axial phase. In the present work we show that in a time-matched plasma focus shot we deduce the value of axial phase current fraction f_c simply by measuring the calibrated voltage waveform and the uncalibrated current waveform. The scaling parameters β and δ are fixed; and by form-fitting the measured current waveform to the normalised current waveform using the value of α of the shot is determined uniquely; from which the peak current and the ratio of peak to average speed [the speed form factor (SFF)] are obtained. The average transit speed is measured by time-of-flight using the voltage upturn as indicator of end of axial phase. Then the SFF yields the peak speed. The measured voltage (back EMF), peak current and peak axial speed (all at the end of axial phase) allows the unambiguous measurement of f_c. The value of the mass swept-up fraction f_m is deduced from α which is the ratio of the characteristic discharge and the characteristic transit times, both deduced during the non-dimensionalisation of the equations. Analysis of a time-matched shot in the INTI PF at 15 kV, 3 Torr D_2 gave $f_c = 0.68$ and $f_m = 0.05$.

Keywords Plasma focus equations · Focus axial phase characteristics · Measurement of model parameters · Plasma focus back EMF

S. Lee · S. H. Saw · V. Damideh
INTI International University, 71800 Nilai, Malaysia

S. Lee · S. H. Saw
Institute for Plasma Focus Studies, 32 Oakpark Drive, Chadstone, VIC 3148, Australia

S. Lee
University of Malaya, Kuala Lumpur, Malaysia

H. Hegazy (✉) · N. Fatis · H. Kariri · A. Khabrani · A. Mahasi
Physics Department, Faculty of Science, Jazan University, 2097 Jazan, Saudi Arabia
e-mail: hossamhegazy@Jazanu.edu.sa

H. Hegazy
Plasma Physics Department, NRC, Atomic Energy Authority, 13759 Inshass, Egypt

J. Ali
Institute of Advanced Photonic Science, Nanotechnology Research Alliance, Universiti Teknologi Malaysia, 81310 Johor Bahru, Malaysia

Introduction

Non-dimensionalising a system of equations is an important technique to obtain characteristic properties of the PF system described by the equations. The normalising or non-dimensionalisation also reduce the parameters of the system to a few scaling parameters [1]. A set of scaling parameters uniquely determines the behaviour of the system.

We apply this important technique to the axial phase of the Mather plasma focus which typically is controlled by

Published online: 05 January 2014

parameters: static inductance L_0, capacitance C_0, stray resistance r_0, anode and cathode radii a and b respectively (or ratio $c = b/a$), anode length z_0 and operational parameters including voltage V_0 and gas pressure and gas type (or density ρ_0) and also current drive fraction f_c and mass swept-up factor f_m [2–5].

In normalising the two coupled equations of motion and circuit for the plasma focus axial phase we reduce the parameters to just three scaling parameters α, β, δ which are the ratios of characteristic times (electrical discharge vs. axial transit), inductances (tube inductance vs. static inductance) and impedances (stray resistance vs. electrical surge impedance) [2, 3]. For each set of α, β, δ there is a unique set of current waveform and trajectory and speed profiles.

To demonstrate the use of this technique, we use the results to analyse an experiment in which we measure the calibrated voltage waveform and the uncalibrated current waveform. From these waveforms we use the characteristic behaviour of the normalised equations and deduce f_c and f_m.

The current drive fraction and mass sept-up fractions are crucial in modeling the plasma focus. There are two pairs: one for the axial phase and one for the radial phase. The present work is discussing the axial phase model parameters.

Experiments had been carried out from time to time by several groups of researchers to determine the fraction of the circuit current flowing into the focus tube and taking part in the driving action on the plasma. The value which is generally accepted is in the range of 0.6–0.7. A method used to measure the plasma current is by placing magnetic probes to detect the magnetic field as the plasma sheath sweeps over the probes [6, 7]. The probe perturbs the plasma changing the flow field and magnetic field patterns sometimes completely changing the flow characteristics especially in smaller plasma focus devices. This method has recently been complemented by using current fitting [4, 8]; to get the values of f_m and f_c by iterative adjustments to the values of f_m and f_c until the axial phase parts of the current traces fit. However the effects of the variations of f_m and f_c are interactive so there is always some uncertainty in this method of fitting [8–11]. A reference value of $f_c = 0.7$ is generally assumed; allowing us to simplify the fitting procedure to a variation of f_m to produce the fit for the axial phase. Then typically only a minor tuning of the value of f_c (about the value of of 0.7) is all that is necessary to produce a good unambiguous fit. So far all the fitting examples have confirmed that using $f_c = 0.7$ as a starting point is consistent with the intensive and extensive study of experimental data for a large range of machines [12–17]. Nevertheless a method of independently finding f_c (without simultaneous adjustments to f_m) is needed to verify the practice of assuming a reference value of $f_c = 0.7$. Through non-dimensionalising the two coupled equations describing the axial phase we deal essentially with one parameter α which allows us to find f_c independently.

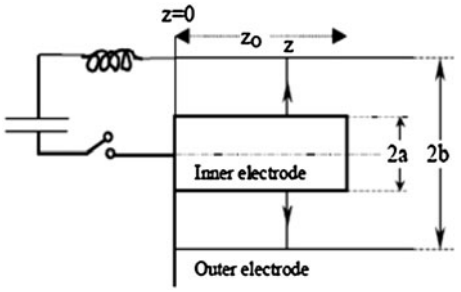

Fig. 1 Schematic of the axial phase of the Mather plasma focus

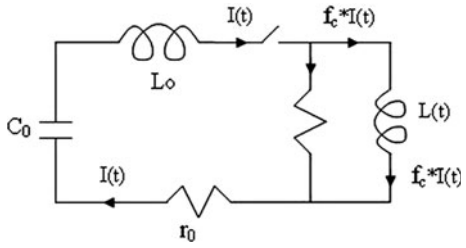

Fig. 2 Plasma focus circuit in the later part of the axial phase: the coaxial tube of the plasma focus up to the axially moving current sheet is treated as a time-dependent inductance L(t) or L_t, neglecting the plasma resistance r_p

Theory

Two Coupled Equations (Motion and Circuit) Describing the Axial Phase

We represent the axial phase of the plasma focus by the schematic shown in Fig. 1. A thin current sheet is driven by the J × B force from postion z = 0 at t = 0 to position z at time t. We use a modified snow-plow model in which the current sheet carrying a fraction f_c of circuit current I at position z has swept up a fraction f_m of the mass it has encountered.

Equating the rate of change of momentum at the current sheet to the driving force averaged across the coaxial channel we have the equation of motion as follows [2, 3]:

$$\rho_0\pi(c^2-1)a^2 f_m \frac{d}{dt}\left(z\frac{dz}{dt}\right) = \frac{\mu f c^2}{4\pi}(\ln c)I^2$$
$$\therefore \frac{d^2z}{dt^2} = \left[\frac{f_c^2}{f_m}\frac{\mu(\ln c)}{4\pi^2\rho(c^2-1)}\left(\frac{I^2}{a}\right)^2 - \left(\frac{dz}{dt}\right)^2\right]\Big/ z \quad (1)$$

Plasma focus axial phase circuit is shown in Fig. 2. The fraction f_c of circuit current I flows in the current sheet with

the rest of the current rendered ineffective shown as flowing through an unlabelled leakage resistance. In the high Magnetic Reynold's number regime [18, 19] where the electromagnetic drive predominates we may ignore the plasma resistance; and the circuit equation may be written as (with the inductance of the coaxial tube $L_t = [\mu/(2\pi)]$ ln(b/a)z where μ is the permeability of the plasma):

$$\frac{d}{dt}[(L_o + Lf_c)I] + r_o I = V_o - \int \frac{Idt}{C_o}$$
$$\frac{dI}{dt} = \left[V_o - \frac{Idt}{C_o} - r_o I - If_c \frac{\mu}{2\pi}(\ln c)\frac{dz}{dt}\right] \Big/ \left[L_o + \frac{f_c \mu}{2\pi}(\ln c)z\right] \quad (2)$$

Equations (1) and (2) are the coupled generating (or governing) equations of this model with interactive effects of the current I and the position z of the current sheet.

Non-dimensionalisation of the Two Coupled Equations

To characterise this set of coupled equations we normalise the equations to obtain the relevant scaling parameters. We replace variables t, z, I by non-dimensionalised quantities as follows:

$$\tau = {}^{t}/_{t_0}, \zeta = z/z, \imath = {}^{I}/_{I_0}$$

where the normalizing quantities t_0, I_0 and z_0 are carefully chosen to be relevant, characteristic, convenient quantities, reflecting the physics of the problem i.e.,$t_0 = \sqrt{L_o C_o}$, z_0 = length of anode and I_0 is V_0/Z_0 where $Z_o = \sqrt{L_o/C_o}$ is the surge impedance (noting that I_o is the peak current of the L_0-C_0 discharge circuit with capacitor C_0 charged initially to V_0 and with $r_0 = 0$).

After non-dimensionalising the Eqs. (1) and (2) may be written as follows:

$$\frac{d^2\zeta}{d\tau^2} = \frac{\left[\alpha^2 \imath^2 - \left(\frac{d\zeta}{d\tau}\right)^2\right]}{\zeta} \quad (3)$$

and

$$\frac{d\imath}{d\tau} = \left(1 - \imath d\tau - \beta\imath\frac{d\zeta}{d\tau} - \delta\imath\right)/(1 + \beta\zeta) \quad (4)$$

where $\alpha = (t_0/t_a)$ with t_a identified as the characteristic axial transit time:

$$t_a = \left[\frac{4\pi^2(c^2-1)}{\mu \ln c}\right]^{1/2} \frac{\sqrt{f_m}}{f_c} \frac{z_o}{(I_o/a)/\sqrt{\rho_o}} \quad (5)$$

$$\beta = \frac{L_a}{L_o} \quad (6)$$

$$\delta = r_o/Z_o \quad (7)$$

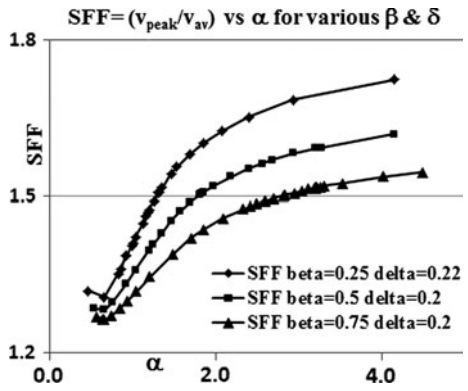

Fig. 3 SFF versus α for various combinations of β (*beta*) and δ (*delta*)

where $L_a = \frac{f_c \mu}{2\pi}(\ln c)z_o$ is the inductance of the plasma focus tube when the current sheet has reached the end of the anode at $z = z_o$.

Some Characteristics of the Electro-dynamics: Uniqueness of Current Profile, Trajectory and Speed Profile of Current Sheet—The Speed Form Factor SFF

Equations (3) and (4) are the non-dimensionalised equivalent of governing Eqs. (1) and (2). Whereas Eqs. (1) and (2) have the parameters b, a, f_c, f_m, ρ_0, V_0, L_0, C_0 with no simple behavioural pattern discernable; in the normalised form Eqs. (3) and (4) can be seen to have behaviour dependant on three ratios of characteristic times (α), inductances (β) and impedances (δ).

For each set of α, β and δ the form of the equations tell us that the profile of current versus time is uniquely different from any other set; as are the profile of distance versus time and speed versus time. This leads to practical applications. As an example we look at the speed form factor (SFF), defined as the ratio of peak axial speed over the average axial speed. Figure 3 shows the SFF as a function of α for three values of β at δ = 0.2.

The value of δ = 0.2 is chosen (δ = 0.22 for the case of β = 0.25 to suit the INTI PF device); as most modern capacitor banks have such a low inherent damping factor. The range of β = 0.25–0.75 covers the range of existing typical machines. The range of α (0.4–4) covers operation of machines reaching the end of axial phase from very early in the discharge (way before the time of peak current) to very late in the discharge (way after time of peak current). Thus Fig. 3 is a valuable tool providing the SFF which allows the peak axial speed to be obtained just from the average transit speed measured by dividing z_0 by the time of the axial phase taken from t = 0 to time of start of the rollover of the current into the dip (or the start of the

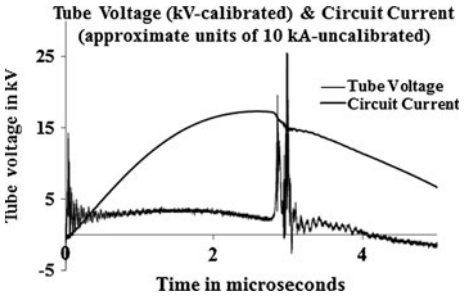

Fig. 4 Time-matched shot in INTI PF at 15 kV 3 Torr D_2. The current trace is the smoother trace and is uncalibrated in current amplitude though we have given it an approximate scale of 10 kA per *vertical unit*

upturn into the voltage spike, see Fig. 4). Moreover for each set of α, β and δ the peak current is also found in non-dimensionalised form which could be immediately converted into the real current by multiplying by I_0.

An Application: Obtaining the Drive Current Fraction f_c of the Axial Phase

We now use this information to obtain the value of f_c for the axial phase of a plasma focus. The value of f_c is an important parameter in the study of electromagnetic shock tubes and the plasma focus alike. Its importance for numerical models has already been discussed in an earlier paragraph as has the importance of verifying its value using a method independent of interaction with f_m.

In this present work we measure the tube calibrated voltage V (inductive back EMF) at the input flanges of the plasma focus together with the uncalibrated current waveform. We choose a time-matched shot in which the end of the axial phase occurs at the time of peak current. For the same shot the average speed of the axial current sheet is measured by time-of-flight and the peak (end axial) speed $(dz/dt)_{peak}$ is obtained by multiplying by a speed form factor obtained from Fig. 3. I_{peak} is also found from the relevant non-dimensionalised current versus time curve. From these measured values of V (at time I_{peak}), I_{peak} and $(dz/dt)_{peak,}$ the value of f_c is determined. The analysis is as follows.

Analysis of the Problem

The circuit of the plasma focus is represented in Fig. 2. The current I enters the plasma focus tube. A fraction f_c (to be determined) of this current creates a current sheet which, interacting with its own magnetic field is accelerated down the coaxial tube, represented in the figure by the inductance L(t). A leakage current flows across the back wall region of the tube and does not take part in the current sheet action. This is represented in the figure by an unlabelled resistance. As the shock wave system develops moving faster and faster, the plasma conductivity rises, the electrical resistance of the current sheet drops. We consider the later part of the axial phase when the axial current sheet has been accelerated to a high speed attaining a high magnetic Reynold's number at which the electromagnetic approximation $r_pI_p(t) \ll d(L(t)I_p(t))/dt$ may be applied. We represent the plasma current as $I_p = f_cI(t)$.

The voltage probe has its high voltage point attached to the anode collector plate and its low voltage point connected to the cathode collector plate of the INTI PF; measuring the voltage V across L(t) also written as L_t we have:

$$V = d\big(L(t)\ I_p(t)\big)/dt$$

$$V = d\big(L_tI_p\big)/dt\ =\ f_cd(L_tI)/dt$$
$$=\ f_cI\ (dL_t/dt)\ +\ f_cL_t(dI/dt)$$

A plasma focus particularly in deuterium, is typically operated with the end of the axial phase occurring at or near peak current so that the radial phase produces the most energetic compression. We may call this mode of operation time-matched. Moreover the current peak is typically relatively gentle so that the condition $dI/dt = 0$ occurs for such time-matched shots. As mentioned earlier we are choosing such a time-matched shot where :

$$V = f_cI\ (dL(t)/dt)$$

For the coaxial geometry of the INTI PF (see section below for INTI PF parameters):

$$L_t = [\mu/(2\pi)]\ln(b/a)\ z \text{ where} \mu = 4\pi10^{-7};\ b/a$$
$$= 3.2/0.95$$

So that $L(t) = 2.4 \times 10^{-7}\ z(t)$ and for the time-matched situation the current and the axial speed are respectively I_{peak} and $(dz/dt)_{peak}$; hence:

$$V = f_c \times I_{peak} \times 2.4 \times 10^{-7} \times (dz/dt)_{peak} \quad (8)$$

The Experiment

For this work we use the INTI PF which is one of the UNU ICTP PFF network machines [18–22]. The configuration parameters are as follows:

Static inductance $L_0 = 114$ nH,
Capacitance $C_0 = 30$ μF,
Circuit resistance $r_0 = 13$ mΩ,
Cathode radius $b = 3.2$ cm,
Anode radius $a = 0.95$ cm,
Anode length $z_0 = 16$ cm,
Voltage $V_0 = 15$ kV, Gas pressure = 3 Torr D_2.

From Eq. (8) we see that to calculate f_c we need the voltage V, the value of I_{peak} and the value of $(dz/dt)_{peak}$ at the time of peak current which corresponds to the end of the axial phase.

For voltage measurements we use a Tektronix high voltage probe P6015A with a rise time of 8 ns and an attenuation factor of 1,000 times. For current measurements we use a 7-turn Rogowski coil which picks up the dI/dt which we then integrate numerically to obtain the current trace [23]. We measure only the current waveform, noting that the calibration constant of a current coil is not very reliable so that we prefer in this experiment to obtain the I_{peak} from the appropriate computed ι versus τ curve chosen by the appropriate α, β and δ combination of the shot. For the value of $(dz/dt)_{peak}$ we first measure the average transit speed of the current sheet by dividing the anode length z_o by the transit time measured from the start of current to the start of the roll-over of the current into the current dip. Then we multiply this average speed by the SFF of the appropriate α, β, δ of the shot.

The scaling parameters β and d for the INTI PF are calculated from known parameters as $\beta = L_a/L_0 = 0.25$ and $\delta = r_0/(L_0/C_0)^{0.5} = 0.22$.

We cannot calculate the primary scaling parameter α since the transit time contains the parameter f_m and f_c which we are trying to find [see Eqs.(4) and (5)]. However we have the measured time profile of the current and we may fit this measured time profile to the various non-dimensionalised current waveforms generated by varying α; with β and δ fixed at 0.25 and 0.22 respectively. Only that current waveform with the correct α will fit the measured current waveform.

Once we have determined the α of our shot we have the appropriate SFF from Fig. 3 from which we deduce $(dz/dt)_{peak}$ using our measured average speed. Also the fitted non-dimensionalised current waveform gives us the appropriate non-dimensionalised current peak from which I_{peak} may be obtained. We have the value of tube voltage V measured with the voltage probe.

Then using Eq. (8) we calculated f_c; and then using Eq. (5) we deduce f_m.

The Results

Figure 4 records the voltage waveform in kV of a time-matched shot in INTI PF at 15 kV 3 Torr D_2. In the same trace is recorded the numerically integrated current waveform from a 7-turn Rogowski-type coil operated as a dI/dt detector. We have found that this coil has sufficiently wide frequency response to faithfully record a plasma focus current waveform [23]. We have a calibration constant for this coil, but for this experiment, as already explained earlier we prefer to obtain the I_{peak} from the non-dimensionalised current trace of the appropriate α, β, δ combination.

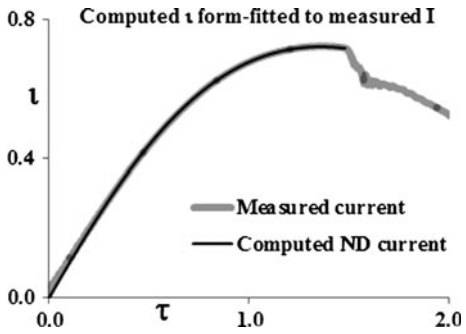

Fig. 5 Fitting the computed non-dimensionalised (ND) current ι waveform to the measured current waveform I by varying α until a good fit is obtained. The best fit (shown in this Figure) was obtained at $\alpha = 1.53$ (with fixed $\beta = 0.25$ and $\delta = 0.22$). The scales are the computed values of ι and τ

Using the measured current waveform (appropriately scaled) as a reference waveform, a non-dimensionalised current waveform is generated with $\beta = 0.25$, $\delta = 0.22$ and α varied from 0.5–2.0.

Each generated waveform is compared by overlaying to an appropriately time- and amplitude-scaled version of the measured current waveform. It was found quickly that for our shot the ranges from $\alpha = 0.5$–1.4 and from 1.7–2.0 shows no possibility of any fit.

The range of $\alpha = 1.4$–1.7 was investigated carefully and a good fit was found in the range of $\alpha = 1.49$–1.58. We decided on an a value of 1.53 ± 0.05 giving (see Fig. 3) a value of SFF range of 1.546 ± 0.01.

The case for $\alpha = 1.53$ is shown in Fig. 5. The small discrepancy near time $\tau = 0$ is always observed in such fitting between measured and computed current traces, due to the imperfect switching and added resistance in the early stages of the discharge which is not modelled. The fit after $\tau = 0.2$ and going on to the end of the axial phase is very good.

From this fit we obtain the peak value of ι as 0.72 which on un-normalising to $I_0 = 243$ kA gives a value of $I_{peak} = 175$ kA.

From the start of the upturn of the voltage trace (Fig. 4) at time $t = 2.65$ μs (confirmed by the start of the roll-over of the current trace) we obtain the average transit speed as 6.04 cm/μs which after multiplying by SFF = 1.546 gives $(dz/dt)_{peak} = 9.3$ cm/μs.

From Fig. 4 we measure the voltage value corresponding to the time of $(dz/dt)_{peak}$ as 2.65 kV.

Thus from Eq. (8) we obtain $f_c = 2{,}650/(175 \times 10^3 \times 2.4 \times 10^{-7} \times 9.3 \times 10^4) = 0.68$.

Then from Eq. (5) we use this value of f_c to compute $f_m = 0.05$.

Conclusion

In this paper we obtained the two coupled equations of motion and circuit describing the trajectory and current profile of the radial phase of the Mather-type plasma focus. We normalised these equations and obtained two coupled equations the behaviour of which depends on three scaling parameters α, β and δ which are ratios of electrical to transit times, inductances and impedances respectively. Thus the behaviour of the axial phase of any plasma focus may be characterised by these 3 parameters. A corollary is that the normalised current waveform, trajectory and speed profile are unique for each combination of α, β, δ. This could lead to important information and insight into various aspects of the axial phase of the plasma focus. As an example we show that in a time-matched plasma focus shot we are able to deduce the value of axial phase current fraction fc simply by measuring the calibrated voltage waveform and the uncalibrated current waveform. The scaling parameters β and δ are fixed for any plasma focus and by form-fitting the measured current waveform to the normalised current waveform, the value of α of the shot is determined uniquely; from which the peak current and SFF of that shot are obtained. The average axial transit speed of the shot is measured by time-of-flight using the current rollover or voltage upturn as indicators of the end of the axial phase. Then the SFF yields the peak speed. The measured voltage, the peak current and the peak axial speed (all at the corresponding time of the peak current, peak axial speed and arrival of current sheet at the end of the anode) allows the measurement of f_c. Once f_c is measured the value of f_m is then deduced from the value of α being the ratio of the characteristic discharge time and the characteristic transit, both of which expressions are deduced during the normalising of the equations. Analysis of a time-matched shot in the INTI PF at 15 kV, 3 Torr D_2 gave a result of $f_c = 0.68$ and $f_m = 0.05$. This determination of these model parameters, especially f_c, using a method which unambiguously fixes the value of f_c is of crucial importance: generally for the fitting of current curves in modelling and particularly for the recent development of novel plasma focus circuits and ideas such as current-steps [24, 25] radiative cooling and collapse [26] and obtaining reference numbers and scaling trends for fast ion beams and fast plasma streams [27, 28].

Acknowledgments Sincere thanks from Jazan University delegation to Prof Ali Alkamli Chair of Physics Dept., and Vice Rector of Jazan University for his kind support and facilitation to perform the present work in Malaysia as well as to P.L. Chong and F. Roy for their assistances during the progress of this work. SL & SHS acknowledge grants INT-CPR-01-02-2012 and FRGS/2/2013/SG02/INTI/01/1.

References

1. http://en.wikipedia.org/wiki/Nondimensionalization. Archival website. Accessed 1 Aug 2013
2. S. Lee, Plasma focus model yielding trajectory and structure, in *Radiations in Plasmas*, vol. 2, ed. by B. McNamara (World Scientific, Singapore, 1984), pp. 978–987
3. S. Lee, Radiative dense plasma focus computation package (RADPF) (2013), http://www.plasmafocus.net/IPFS/modelpackage/File2Theory.pdf. Archival website. Accessed 1 Aug 2013
4. S.H. Al-Hawat, M. Akel, S. Lee, S.H. Saw, Model parameters vs gas pressure in two different plasma focus devices operated in argon and neon. J. Fusion Energ. **31**, 13–20 (2012). doi:10.1007/s10894-011-9414-3
5. T.Y. Tou, S. Lee, K.H. Kwek, Nonperturbing plasma-focus measurements in the run-down phase. IEEE Trans. Plasma Sci. **17**(2), 311–315 (1989)
6. T. Oppenländer. Ph.D. Dissertation, University of Stuttgart, Germany (1981)
7. L. Flemming, H.J. Kaeppeler, T. Oppenlander, G. Pross, P. Schilling, H. Schmidt, M. Shakhatre, M. Trunk, Plasma Phys. **22**, 245–260 (1980)
8. S. Lee, S.H. Saw, P.C.K. Lee, R.S. Rawat, H. Schmidt, Computing plasma focus pinch current from total current measurement. Appl. Phys. Lett. **92**, 111501 (2008)
9. S.H. Saw, S. Lee, Scaling laws for plasma focus machines from numerical experiments. Energy Power Eng. **1**, 65–72 (2010)
10. S.H. Saw, S. Lee, Scaling the plasma focus for fusion energy considerations. Int. J. Energy Res. **35**, 81–88 (2011)
11. S. Lee, S.H. Saw, A.E. Abdou, H. Torreblanca, Characterising plasma focus devices—role of static inductance–instability phase fitted by anomalous resistance. J. Fusion Energ. **30**, 277–282 (2011)
12. S. Lee, Neutron yield saturation in plasma focus—a fundamental cause. Appl. Phys. Lett. **95**, 151503 (2009)
13. S. Lee, R.S. Rawat, P. Lee, S.H. Saw, Soft x-ray yield from NX2 plasma focus. J. Appl. Phys. **106**, 023309 (2009)
14. S.H. Saw, P.C.K. Lee, R.S. Rawat, S. Lee, Optimizing UNU/ICTP PFF plasma focus for neon soft X-ray operation. IEEE Trans. Plasma Sci. **37**, 1276–1282 (2009)
15. S. Lee, S.H. Saw, Neutron scaling laws from numerical experiments. J. Fusion Energ. **27**, 292–295 (2008)
16. S. Lee, S.H. Saw, L. Soto, S.P. Moo, S.V. Springham, Numerical experiments on plasma focus neutron yield versus pressure compared with laboratory experiments. Plasma Phys. Control. Fusion. **51**, 075006 (2009)
17. M. Akel, S. Lee, S.H. Saw, Numerical experiments in plasma focus operated in various gases. IEEE Trans. Plasma Sci. **40**(12), 3290 (2012). doi:10.1109/TPS.2012.2220863
18. S. Lee, S.H. Saw, P.C.K. Lee, R.S. Rawat, K. Devi, Magnetic reynolds number and neon current sheet structure in the axial phase of a plasma focus. J. Fusion Energ. **32**(1), 50–55 (2012)
19. S.H. Saw, M. Akel, P.C.K. Lee, S.T. Ong, S.N. Mohamad, F.D. Ismail, N.D. Nawi, K. Devi, R.M. Sabri, A.H. Baijan, J. Ali, S. Lee, Magnetic probe measurements in INTI plasma focus to determine dependence of axial speed with pressure in neon. J. Fusion Energ. **31**, 411–417 (2012)
20. S. Lee, S.H. Saw, R.S. Rawat, P. Lee, A. Talebitaher, A.E. Abdou, P.L. Chong, F. Roy, A. Singh, D. Wong, K. Devi, Correlation of soft x-ray pulses with modeled dynamics of the plasma focus. IEEE Trans. Plasma Sci. **39**(11), 3196–3202 (2011)
21. S.H. Saw, S. Lee, F. Roy, P.L. Chong, V. Vengadeswaran, A.S.M. Sidik, Y.W. Leong, A. Singh, In-situ determination of the

static inductance and resistance of a plasma focus capacitor bank. Review Sci Instrum. **81**(053505) (2010)
22. S. Lee, T.Y. Tou, S.P. Moo, M.A. Elissa, A.V. Gholap, K.H. Kwek, S. Mulyodrono, A.J. Smith, Suryadi, W. Usala, M. Zakaullah, A simple facility for the teaching of plasma dynamics and plasma nuclear fusion. Am. J. Phys. **56**, 62 (1988)
23. S. Lee, S.H. Saw, R.S. Rawat, P. Lee, R. Verma, A. Talebitaher, S.M. Hassan, A.E. Abdou, Mohamed Ismail, Amgad Mohamed, H. Torreblanca, S.H. AlHawat, M. Akel, P.L. Chong, F. Roy, A. Singh, D. Wong, K. Devi, Measurement and processing of fast pulsed discharge current in plasma focus machines. J. Fusion Energ. **31**, 198–204 (2012)
24. S.H. Saw, Experimental studies of a current-stepped Pinch PhD Thesis University of Malaya, Malaysia (1991)
25. S. Lee, S.H. Saw, Current-step technique to enhance plasma focus compression and neutron yield. J. Fusion Energ. **31**, 603–610 (2012)
26. S. Lee, S.H. Saw, J. Ali, Numerical experiments on radiative cooling and collapse in plasma focus operated in krypton. J. Fusion Energ. **32**, 42–49 (2013)
27. S. Lee, S.H. Saw, Plasma focus ion beam fluence and flux—scaling with stored energy. Phys. Plasmas **19**, 112703 (2012)
28. S. Lee, S.H. Saw, Plasma focus ion beam fluence and flux—for various gases. Phys. Plasmas **20**, 062702 (2013)